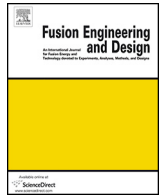




Contents lists available at ScienceDirect

Fusion Engineering and Design

journal homepage: www.elsevier.com/locate/fusengdes



Development of a high energy pulsed plasma simulator for the study of liquid lithium trenches

S. Jung^{a,*}, M. Christenson^a, D. Curreli^a, C. Bryniarski^b, D. Andruczyk^{a,1}, D.N. Ruzic^a

^a Department of Nuclear, Plasma, and Radiological Engineering, University of Illinois at Urbana-Champaign, Urbana 61801, USA

^b Department of Electrical and Computer Engineering, University of Illinois at Urbana-Champaign, Urbana 61801, USA

HIGHLIGHTS

- A pulse device for a liquid lithium trench study is developed.
- It consists of a coaxial plasma gun, a theta pinch, and guiding magnets.
- A large energy enhancement is observed with the use of the plasma gun.
- A further increase in energy and velocity is observed with the theta pinch.

ARTICLE INFO

Article history:

Received 6 December 2013

Accepted 24 February 2014

Available online xxx

Keywords:

Liquid lithium

Plasma–wall interaction

Pulsed plasma source

Plasma gun

Theta pinch

ABSTRACT

To simulate detrimental events in a tokamak and provide a test-stand for a liquid-lithium infused trench (LiMIT) device [1], a pulsed plasma source utilizing a theta pinch in conjunction with a coaxial plasma accelerator has been developed. The plasma is characterized using a triple Langmuir probe, optical methods, and a calorimeter. Clear advantages have been observed with the application of a coaxial plasma accelerator as a pre-ionization source. The experimental results of the plasma gun in conjunction with the existing theta pinch show a significant improvement from the previous energy deposition by a factor of 14 or higher, resulting in a maximum energy and heat flux of 0.065 ± 0.002 MJ/m² and 0.43 ± 0.01 GW/m². A few ways to further increase the plasma heat flux for LiMIT experiments are discussed.

© 2014 Elsevier B.V. All rights reserved.

1. Introduction

Plasma–wall interactions in a tokamak have become significant issues as energy in tokamak plasmas has increased and detrimental events, such as edge-localized modes, were discovered. These violent events occur on a very short timescale, typically over a few hundred microseconds to milliseconds, resulting in a huge amount of power bombarding the target. For example, typical energies of ELMs (edge-localized modes) are about 0.01–0.05 MJ/m² for ASDEX-upgrade, 0.1–0.5 MJ/m² for JET and is expected to be 1–5 MJ/m² for ITER [2]. A recent report says that ITER will not be able to tolerate damage to its plasma facing components unless ELMs can be eliminated or reduced in magnitude by 95% [3] and the peak energy density must be smaller than 0.5 MJ/m² to have a

lifetime of 10^7 thermal pulses of 500 μs duration [4]. Therefore, a major part of the tokamak research effort is aiming toward the development of physics and technologies to cope with these extreme events including (1) mitigation of ELM events such as resonance magnetic perturbation [5] and (2) studies of plasma–wall interactions at high levels of heat flux [28–30].

A recent study at the University of Illinois [1] shows that a heat gradient between the front and back surfaces of a liquid metal can be coupled with an external magnetic field to generate a thermo-electric magneto-hydrodynamic (TEMHD) force. This configuration, with a slit-shaped electron beam source implemented to create a heat gradient within the trench, removes a peak heat flux of 3 MW/m², and has the potential of removing up to 20 MW/m² [1]. This concept is a good candidate as a plasma facing component, not only because lithium displays several beneficial effects such as less radiation losses than carbon and tungsten, a better gettering of carbon and oxygen, and a lower recycling coefficients [6,7], but also because the liquid lithium can be replenished by the TEMHD force.

An unexplored part of the work related with the LiMIT device is how the trenches will behave with a larger amount of heat flux

* Corresponding author. Tel.: +1 217 333 1568.

E-mail addresses: jung73@illinois.edu, jungsoonw@gmail.com (S. Jung).

¹ The author is currently on assignment at Princeton Plasma Physics Lab, MS41, P.O. Box 451, Princeton, NJ 08543-08540, USA.

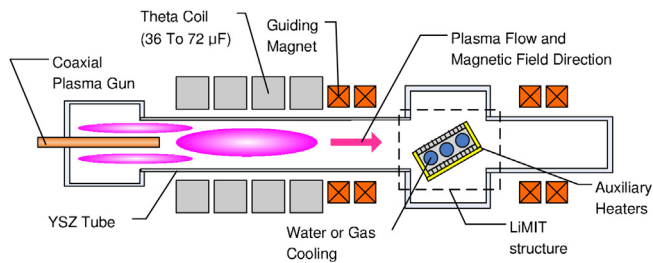


Fig. 1. A diagram of the TELS device. While the LiMIT structure is not tested in this paper, the structure is added to the figure for readers to understand the final experimental setup.

on a shorter time scale ($\sim 100 \mu\text{s}$). In order to further investigate in detail the feasibility of the lithium-trench as a plasma facing component, a new project entitled thermoelectric-driven liquid metal plasma facing structures (TELS) has started. For this project, we are mainly focusing on two subtasks: (1) develop and refine the geometry of new thermo-electric driven structures to handle higher heat flux and (2) develop a laboratory-scale experiment to simulate off-normal events in tokamak devices and to test the trenches in those environments. This paper presents mainly the development of a small-size ($\leq 2 \text{ m}$ in length) pulsed-plasma heat load simulator to investigate the short-pulse effect on the liquid lithium infused trenches.

In this paper, development of a pulsed plasma source using a theta pinch in conjunction with a coaxial plasma gun for LiMIT device testing is presented. In Section 2, the principal elements of the device and experiment, including a description of the physical components as well as the electrical circuit and diagnostics, will be described. In Section 3, initial experimental results such as plasma density, electron temperature, plasma heat flux, and plasma velocity are presented. In Section 4, the results are summarized and concluded with future directions for further improvement.

2. TELS description

There are numerous works that aim toward the development of laboratory-scale energetic plasma generators to simulate and study the interaction between plasma and plasma-facing components [8–16]. A distinctive feature of the new device described in this paper is the use of the existing theta pinch at the University of Illinois [17–19] to allow for an additional control of ion temperature [20]. New additions to the existing pinch device include a coaxial plasma gun and guiding magnets for plasma creation, acceleration, and transport to the target region. A diagram of the initial experimental setup is shown in Fig. 1. The device is planned to be further modified to implement a liquid lithium-infused trench device and other equipments, including an electron beam for initial heating of LiMIT and electron beam focusing magnets. In summary, the device aims at achieving $n_e \geq 10^{21} \text{ m}^{-3}$, $T_{i+e} \sim 100 \text{ eV}$, $v \sim 50 \text{ km/s}$, and a plasma heat flux $\sim 0.1 \text{ MJ/m}^2$ in 100–200 μs .

2.1. Plasma gun

The coaxial plasma gun is used to create a high density plasma and provide it with an axial momentum through a Lorentz force. Oxygen-free copper has been chosen as an electrode material for initial testing. The cathode is an oxygen-free copper cylindrical rod with a 1 in. outer diameter and 12 in. length. An existing 8 in. stainless CF nipple serves as an anode, since it minimizes modification of the device. The inner diameter of the chamber is 6 in. and the length is 15 in. This setup gives an inductance of approximately 0.1 μH . A

500 μF capacitor with a maximum voltage of 10 kV is charged up to 6 kV ($= 9 \text{ kJ}$) and discharged through a T-508 spark gap switch and 10 RG-217 cables. Hydrogen gas is fed by a Parker series 9 pulse valve from the end of the chamber. In most experimental cases, the plenum pressure is between 35 and 100 psi, which gives approximately 130–300 mTorr of gas pressure in the chamber. The base pressure in the chamber is 10^{-7} Torr.

2.2. Theta pinch and guiding magnets

Conventional resonance-type wave heating is not an effective way to heat the plasma from the gun since the plasma lasts for a very short time ($\leq 150 \mu\text{s}$) and the temporally changing plasma parameters result in difficulties in coupling and matching. Therefore, the theta pinch is a good alternative to heat the plasma given the current experimental setup. For example, 10 kJ of capacitor energy discharged in 100 μs with an energy transfer efficiency of 10% results in 10 MW of electric power. Therefore, the theta pinch provides a simple way to heat the plasma. A pyrex tube is surrounded by a conical theta coil (#12 μ 13#) which is connected by 15 LDF5-50A Heliac cables to a 72 μF capacitor bank. The capacitor bank has been upgraded from 36 μF bank to increase the stored energy in the bank and to facilitate a crowbar operation. While the capacitor bank can be ideally charged up to a maximum of 60 kV, experiments are carried out under 20 kV ($= 14.4 \text{ kJ}$) due to limitations on the railgap switch and high voltage insulation issues.

We have two magnets at the target chamber. Guiding magnets initially serve to simulate an external toroidal magnetic field for LiMIT the trench. At the same time, the magnets also suppress expansion of the plasma after the plasma is ejected from the theta coil. While the magnets are supposed to ideally generate a long pulse to drive the liquid lithium flow, the magnets are powered by separate capacitor banks through 50RIA60 SCR switches for the purpose of this paper. Peak magnetic fields of 0.30 T from the magnet between the theta coil and the chamber and 0.15 T from the magnet at the end of the target chamber are generated. A 316 stainless steel magnetic flux excluder is inserted between the theta coil and the guiding magnetic field to decouple magnetic fields from each other. It turns out that the voltage of the capacitor for the magnet next to the theta coil is perturbed only by the maximum of 2 V during the main bank discharge.

2.3. Diagnostics

Since the plasma lasts for approximately 150–200 μs and the density and temperature changes relatively fast, this experimental condition allows for very limited choices in diagnostics. Here, we use a triple Langmuir probe [21] to measure the plasma density and electron temperature. The triple Langmuir probe data is sensitive to noise and small changes in the signal at high electron temperature. This is more severe when the probe is not saturated; therefore, error propagation is taken into account for the analysis. Many different types of circuits for biasing the probe have been tested. The triple probe current is measured by a 4100 Pearson coil and the voltages at the tips are measured by two P5200 Tektronix high voltage differential probes. The probe is oriented parallel to the tube to reduce the plasma velocity effect.

We have also manufactured a calorimeter to estimate the incoming plasma energy. A button-type calorimeter, similar to those in [22,23], made of copper with a 6.4 mm. diameter and with a 5 mm length is used. The copper is insulated with Macor ceramics on all sides except the front surface. A K-type thermocouple is attached to the back surface of the copper and the thermocouple is connected to a computer through a U-3 Labjack interface to record the rise in temperature. The calorimeter is located at the target region, approximately 30 in. away from the plasma gun.

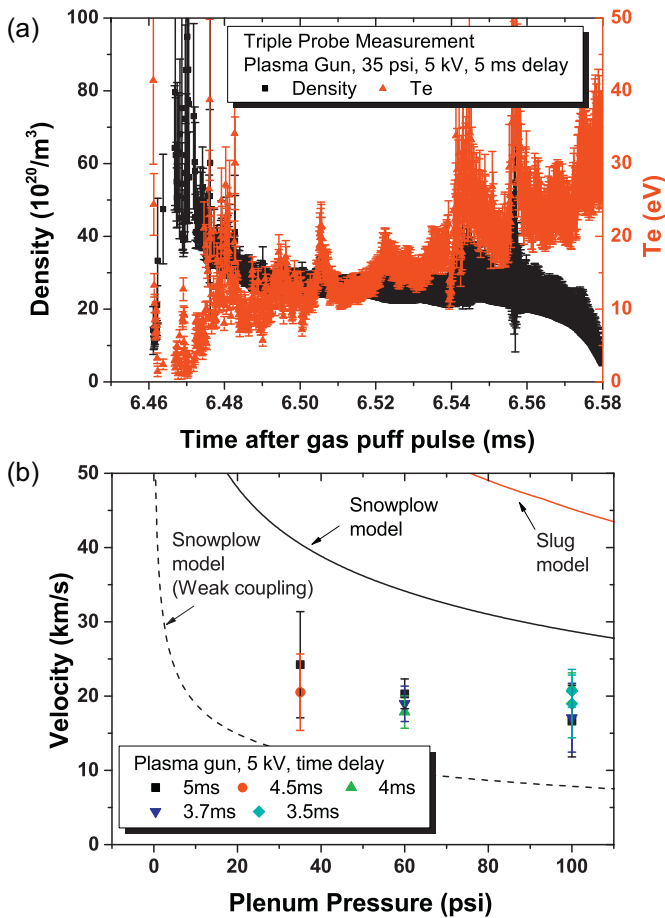


Fig. 2. (a) temporal change of plasma density and electron temperature at the center of the theta coil. The black dot and line refer to plasma density and the red dot and line indicate electron temperature. (b) measurement of the plasma velocity at the end of the plasma gun. The red solid line is a prediction of the velocity from a slug model, the black solid line is from a snowplow model, and the dashed line is from a weakly coupled snowplow model. (For interpretation of the references to color in this figure legend, the reader is referred to the web version of this article.)

In order to measure the plasma velocity, we use a time of flight technique with two high bandwidth PDA 100A photodiodes. The two photodiodes at two different locations measure the time that it takes for the plasma to travel and the time is converted to a velocity. To maximize the bandwidth, the photodiodes are operated with no gain. The diodes are placed at the end of the gun for velocity measurement of the plasma from the plasma gun. For measuring the plasma velocity after the pinch, the diodes are relocated between the theta coil and the guiding magnets.

3. Initial results

3.1. Plasma parameter measurements for the plasma gun

Fig. 2(a) shows a plot of the temporal change of the plasma density and electron temperature produced by the plasma gun at 5 kV. The density and temperature are measured at the center of the theta coil using a triple Langmuir probe. Typical density measurements are around 10^{21} m^{-3} and electron temperature measurements of 10–30 eV.

Fig. 2(b) shows a plot of plasma velocities at different plenum pressures and at different timings between the gas puff and plasma gun. A velocity of 15–30 km/s is obtained. The measured velocities are similar to those predicted by the two different theoretical approaches of the slug model [24,25] and are similar to those

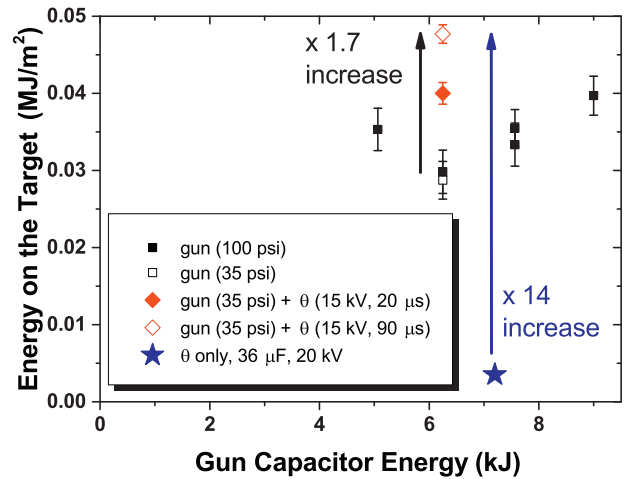


Fig. 3. plasma heat flux measured using the calorimeter. The black square dot is data from a plasma gun at 5 kV, the red diamond dots are from the plasma gun and the theta pinch with 100 μs delay (solid dot) and 200 μs (empty dot). The blue star dot is the data from previous data in ref. [19]. This data is added for comparison with the current data. (For interpretation of the references to color in this figure legend, the reader is referred to the web version of this article.)

predicted by the two different theoretical approaches of the weakly - coupled snowplow model [31] and the snowplow model [26].

3.2. Plasma heat flux measurements for plasma gun and theta pinch

Fig. 3 shows a plot of plasma energy versus the capacitor energy. Note that for the data obtained by the combined operation of the plasma gun and the theta pinch, the energy in the capacitor for the theta pinch is not included in the capacitor energy at the x axis of Fig. 3. Note also that the timing delay in Fig. 3 refers to the delay between the triggering signal of the plasma gun and that of theta pinch, and it is not the same as the actual delay due to the relatively large jitter from the plasma gun.

Using a button-type calorimeter, the plasma accelerated using the plasma gun was found to have a peak energy flux of 0.04 MJ/m^2 . Testing the theta pinch at two different timings, a maximum energy enhancement of a factor of 1.7 compared with the plasma gun alone is obtained at the same preionization capacitor voltage. Further experiments reveal that the energy enhancement with the theta pinch is normally a factor of 1.5. This energy enhancement is a large improvement from the previous theta pinch device, showing an increase in the energy by a factor of 10 or more compared to the energy obtained using the same theta pinch and a $36 \mu\text{F}$ capacitor bank at 20 kV [19]. Further experiments show that using a 15 kV charge on the theta pinch and a 6 kV charge on the plasma gun produces a maximum energy deposition of $0.065 \pm 0.002 \text{ MJ/m}^2$ and a maximum heat flux of $0.43 \pm 0.01 \text{ GW/m}^2$ in 150 μs pulse.

Fig. 4(a) shows the change of the current at the theta coil when the crowbar is fired. The crowbar is not fired when the delay time is equal to or greater than 5 μs . Therefore, the time delay between the main switch and the crowbar is fixed at 4 μs . As shown in Fig. 4(a), the current remains positive for 100 μs .

Fig. 4(b) shows the plasma heat flux as a function of delay time between the plasma gun and the theta pinch at a plenum pressure of 35 psi. The plenum pressure is reduced from 100 psi to increase the efficiency of pinching. Here, the theta coil is reconfigured to a two-turn coil for crowbar operation since the crowbar switch has a finite inductance of approximately 100 nH. The data in Fig. 4(b) show that the energy is further increased by the theta pinch and the guiding magnet. While the energy with the guiding magnets is similar to the energy without the magnets, it is advantageous since the guiding

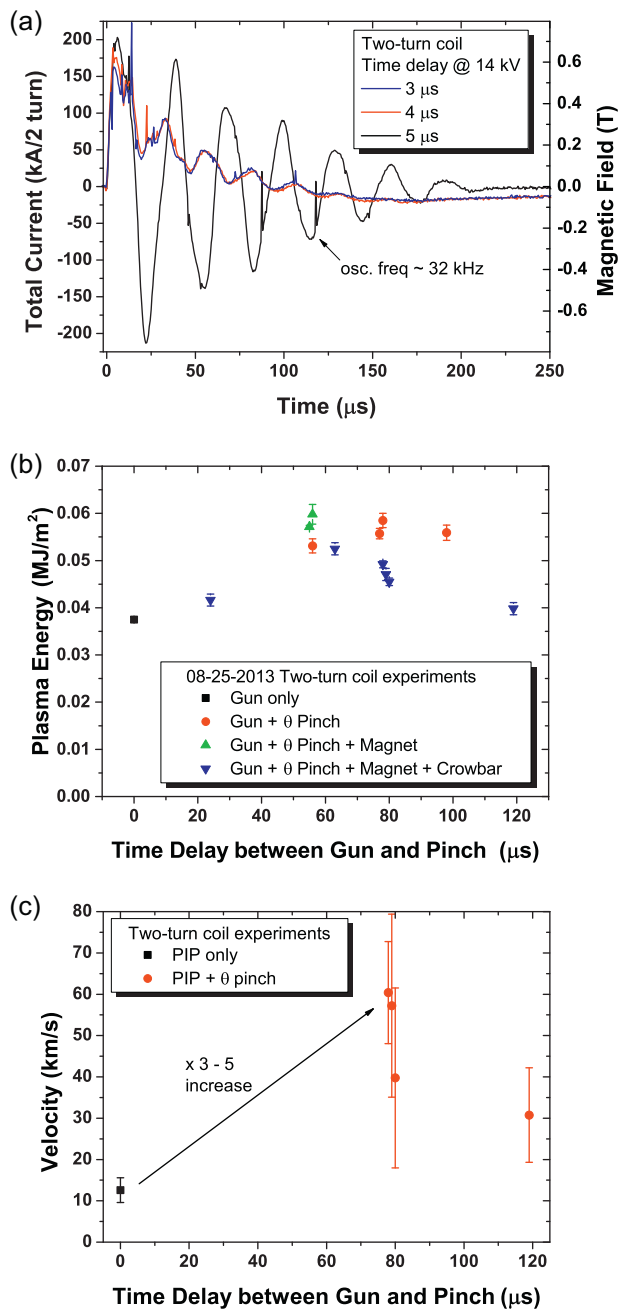


Fig. 4. (a) the current trace at the theta coil with and without the crowbar (b) plasma heat flux measured using the calorimeter for the operation of the plasma gun at 5 kV and the theta pinch at 15 kV. The black square dot is data from only the plasma gun. The red circle dot is from the plasma gun and the theta pinch. The green triangular dot is the data from the guiding magnetic fields as well as the plasma gun and the theta pinch. The inverted triangular blue dot is the data from a full operation of the device, including the crowbar, the guiding magnetic fields, the theta pinch as well as the plasma gun. (c) velocity measured using a time of flight technique. (For interpretation of the references to color in this figure legend, the reader is referred to the web version of this article.)

magnetic field actually decreases the plasma energy by 25–30% for the case of using only the plasma gun. For the plasma gun case, the magnetic field provides a magnetic pressure, preventing the plasma from translating to the target region. However, for the plasma gun and the pinch case the guiding magnetic field (~0.30 T) is weaker than the theta coil field (~0.80 T), so the guiding magnetic field serves to help reduce the radial transport. This data is beneficial in that the magnetic field for LiMIT does not significantly reduce the plasma heat flux when operated with the pinch. While the crowbar

ideally prevents magnetic field reversal between the theta pinch and the guiding magnets and transport the plasma more efficiently, the crowbar itself consumes additional energy from the capacitor bank and the theta pinch compresses the plasma only once so that the total energy is actually reduced.

Fig. 4(c) shows the velocity of the plasma with the plasma gun and the theta pinch. The photodiodes are placed at the end of the theta coil for the measurement. Since the plasma velocity changes with the pinching process the velocity is not easily determined by a single value so that the velocity has a relatively large deviations. However, it is found that the velocity is increased by a factor of 3–5 with pinching and the velocity reaches around 40–60 km/s on average.

4. Conclusions and future directions

As part of an effort to develop a pulsed plasma simulator to simulate fusion-relevant plasma and to provide a test-stand for the liquid-lithium infused trenches device, the existing theta pinch operation has been modified to be equipped with a coaxial plasma gun and guiding magnets. A density of 10^{21} m^{-3} , electron temperature of 10–30 eV, and the velocity of 10–30 km/s are obtained with the coaxial plasma gun. The theta pinch allows for approximately a factor of 1.5 increase over the plasma gun alone and the combination of the plasma gun and theta pinch produce an order of magnitude enhancement as compared to results before the upgrade [17,19], with a maximum energy and heat flux of $0.065 \pm 0.002 \text{ MJ/m}^2$ and $\sim 0.43 \pm 0.01 \text{ GW/m}^2$.

We are currently working on increasing the energy at the theta pinch capacitor bank up to 20 kV or higher to further compress the preionized plasma. At the same time, several diagnostics, including a retarding field energy analyzer [27] are being developed and tested to further investigate the effect of pinching on the plasma from the plasma gun as well as determine the overall effect of the guiding magnetic field. Increasing bank voltages and upgrading to higher voltage hardware will allow us to achieve a plasma heat flux up to 0.1 MJ/m^2 . Once this condition is achieved, the device will be equipped with the LiMIT to test and measure lithium–vapor shielding effect.

Acknowledgments

The research reported in this paper was performed in support of contract number DE-SC0008587 with the U.S. Department of Energy. The author would like to thank M. Williams for numerous technical discussions and undergraduate researchers H. Yun, A. Lietz, B. Lee, M. Pace, and M. Sullivan for their time and commitment in the laboratory.

References

- [1] D. Ruzic, W. Xu, D. Andruczyk, M. Jaworski, Lithium-metal infused trenches (limit) for heat removal in fusion devices, *Nuclear Fusion* 51 (2011) 102002.
- [2] D. Naujoks, Plasma–Material Interaction in Controlled Fusion, Springer, Berlin, 2006, p. 144.
- [3] D.P. Boyle, R. Maingi, P.B. Snyder, J. Manickam, T.H. Osborne, R.E. Bell, et al., The relationships between edge localized modes suppression, pedestal profiles and lithium wall coatings in NSTX, *Plasma Physics and Controlled Fusion* 53 (2011) 105011.
- [4] P.R. Thomas, ELM physics and ELM mitigation in ITER, Presented at the 22nd IAEA Fusion Energy Conference, Geneva, Switzerland, 2008.
- [5] T.E. Evans, R.A. Moyer, K.H. Burrell, M.E. Fenstermacher, I. Joseph, A.W. Leonard, et al., Edge stability and transport control with resonant magnetic perturbations in collisionless tokamak plasmas, *Nature Physics* 2 (2006) 419–423.
- [6] M. Baldwin, R. Doerner, S. Luckhardt, R. Conn, Deuterium retention in liquid lithium, *Nuclear Fusion* 42 (2002) 1318.
- [7] R. Majeski, S. Jardin, R. Kaita, T. Gray, P. Marfuta, J. Spaleta, et al., Recent liquid lithium limiter experiments in CDX-U, *Nuclear Fusion* 45 (2005) 519.

- [8] V. Belan, V. Levashov, V. Maynashev, A. Muzichenko, V. Podkovirov, Features of dynamics and structure of the shielding layer at the interaction of plasma flow with target, *Journal of Nuclear Materials* 233–237 (Part 1) (1996) 763–766.
- [9] V. Safronov, N. Arkhipov, I. Landman, S. Pestchanyi, D. Toporkov, A. Zhitlukhin, Evaporation and vapor shielding of CFC targets exposed to plasma heat fluxes relevant to ITER ELMs, *Journal of Nuclear Materials* 386–388 (2009) 744–746.
- [10] I.E. Garkusha, N.I. Arkhipov, N.S. Klimov, V.A. Makhilaj, V.M. Safronov, I. Landman, et al., The latest results from ELM-simulation experiments in plasma accelerators, *Physica Scripta* 2009 (2009) 014054.
- [11] Y. Kikuchi, R. Nakanishi, M. Nakatsuka, N. Fukumoto, M. Nagata, Characteristics of magnetized coaxial plasma gun for simulation experiment of thermal transient events in ITER, *IEEE Transactions on Plasma Science* 38 (2010) 232–236.
- [12] G.D. Temmerman, J. Zielinski, S. van Diepen, L. Marot, M. Price, ELM simulation experiments on pilot-PSI using simultaneous high flux plasma and transient heat/particle source, *Nuclear Fusion* 51 (2011) 073008.
- [13] B. de Groot, Z. Ahmad, R. Dahiya, R. Engeln, W. Goedheer, N.L. Cardozo, et al., Magnum-PSI, a new linear plasma generator for plasma–surface interaction studies in ITER relevant conditions, *Fusion Engineering and Design* 66–68 (2003) 413–417.
- [14] H.J.N. van Eck, in: Ph.D. dissertation, Technische Universiteit Eindhoven, 2013.
- [15] Y. Hirooka, R.W. Conn, T. Sketchley, W.K. Leung, G. Chevalier, R. Doerner, et al., A new plasma–surface interactions research facility: PISCES-B and first materials erosion experiments on bulk-boronized graphite, *Journal of Vacuum Science & Technology A: Vacuum, Surfaces, and Films* 8 (1990) 1790–1797.
- [16] J. Rapp, Status of R&D for the planned material plasma exposure experiment (MPEX), Presented at the 4th International Workshop on Plasma Material Interaction Facilities for Fusion Research, Oak Ridge, Tennessee, USA, 2013.
- [17] T.K. Gray, in: Ph.D. dissertation, University of Illinois at Urbana–Champaign, 2009.
- [18] S. Jung, V. Surla, T. Gray, D. Andruczyk, D. Ruzic, Characterization of a theta-pinch plasma using triple probe diagnostic, *Journal of Nuclear Materials* 415 (2011) S993–S995.
- [19] S. Jung, D. Andruczyk, D. Ruzic, Laboratory investigation of vapor shielding for lithium-coated molybdenum in DEVeX, *IEEE Transactions on Plasma Science* 40 (2012) 730–734.
- [20] K. Miyamoto, *Plasma Physics for Nuclear Fusion*, revised ed., MIT Press, Cambridge, MA, 1976, pp. 441–443.
- [21] S.-L. Chen, T. Sekiguchi, Instantaneous direct-display system of plasma parameters by means of triple probe, *Journal of Applied Physics* 36 (1965) 2363–2375.
- [22] S. Suzuki, J.F. Crawford, J.T. Bradley III, J.M. Gahl, R. Nygren, Experimental study of pulse plasma heat flux absorption and ablation during the simulation of a tokamak plasma disruption, *Journal of Nuclear Materials* 200 (1993) 265–269.
- [23] N.F.M. Nagata, Y. Kikuchi, Application of magnetized coaxial plasma guns for simulation of transient high heat loads on ITER divertor, *IEEE Transactions on Electrical and Electronic Engineering* 4 (1999) 518–522.
- [24] P.M. Mostov, J.L. Neuringer, D.S. Rigney, Electromagnetic acceleration of a plasma slug, *Physics of Fluids* (1958–1988) 4 (1961) 1097–1104.
- [25] P.J. Hart, Plasma acceleration with coaxial electrodes, *Physics of Fluids* (1958–1988) 5 (1962) 38–47.
- [26] K.J. Chung, K.S. Chung, Y.S. Hwang, Characteristics of rail gun plasma as a small-scale ELM simulator, Presented at the 25th Symposium on Fusion Engineering, San Francisco, California, USA, 2013.
- [27] M. Christenson, S. Jung, D. Andruczyk, D. Curreli, D.N. Ruzic, Measuring the ion energy distribution using a retarding field energy analyzer in a plasma material interaction test stand, Presented at the 55th Annual Meeting of the APS Division of Plasma Physics, Denver, Colorado, USA, 2013.
- [28] V.A. Evtikhin, I.E. Lyublinski, A.V. Vertkov, V.G. Belan, I.K. Konkashbaev, L.B. Nikandrov, Calculation and experimental investigation of fusion reactor divertor plate and first wall protection by capillary-pore systems with lithium, *Journal of Nuclear Materials* vol. 271–272 (1999) 396–400.
- [29] N.V. Antonov, V.G. Belan, V.A. Evtihin, L.G. Golubchikov, V.I. Khripunov, V.M. Korjavin, I.E. Lyublinski, V.S. Maynashev, V.B. Petrov, V.I. Pistunovich, V.A. Pozharov, V.I. Podkovirnov, V.V. Shapkin, A.V. Vertkov, Experimental and calculated basis of the lithium capillary system as divertor material, *Journal of Nuclear Materials* vol. 241–243 (1999) 1190–1196.
- [30] I.E. Lyublinskia, A.V. Vertkova, V.A. Evtikhin, Application of lithium in systems of fusion reactors. 2. The issues of practical use of lithium in experimental facilities and fusion devices, *Plasma Devices and Operations* vol. 17 (2009) 265–285.
- [31] D. Dietz, Coaxial plasma accelerator in the snowplow mode: analytical solution in the weak coupling limit, *Journal of Applied Physics* 62 (1987) 2669–2674.